

# Perstraction of Heat-Stable Salts from Aqueous Alkanolamine Solutions

M. I. Kostyanaya<sup>a</sup>, A. A. Yushkin<sup>a</sup>, D. S. Bakhtin<sup>a</sup>, S. A. Legkov<sup>a</sup>, and S. D. Bazhenov<sup>a,\*</sup>

<sup>a</sup> *Topchiev Institute of Petrochemical Synthesis, Russian Academy of Sciences, Moscow, 119991 Russia*

\**e-mail: sbazhenov@ips.ac.ru*

Received December 12, 2021; revised November 8, 2022; accepted December 1, 2022

**Abstract**—Amine absorption processes designed to remove acid gases from gas streams generally face a major challenge of solvent degradation. This degradation leads to the formation of heat-stable salts (HSS), corrosive agents that irreversibly bind free alkanolamine. The present study proposes, for the first time, a method for HSS perstraction using a liquid–liquid membrane contactor that allows HSS to transfer through porous membranes from the solvent into a hydrophobic extractant represented by a methyltrioctylammonium solution in 1-octanol. The perstraction provides selective extraction of HSS anions without direct mixing of liquid phases or the formation of stable emulsions of the solvent and the extractant. For this purpose, a number of industrial and laboratory porous membrane samples fabricated from polyvinylidene fluoride, polypropylene, and polysulfone were investigated. Their chemical and morphological stability, surface properties, and transport properties were tested under prolonged (>600 h) contact with a model solvent (an aqueous monoethanolamine solution) and with the components of the selective extractant. The feasibility of HSS perstraction was demonstrated using the formic acid (as an HSS model) extraction from the model solvent. The most promising results were obtained for a system with a polyvinylidene fluoride membrane: up to 50% of formic acid was extracted over 18 h.

**Keywords:** perstraction, heat-stable salts, liquid–liquid membrane contactor, selective extractant, alkanolamines, carbon dioxide, absorption

**DOI:** 10.1134/S0965544122100097

## INTRODUCTION

Along with mechanical treatment and dehydration, removing acid gases such as carbon dioxide (CO<sub>2</sub>) and hydrogen sulfide (H<sub>2</sub>S) is a critical process step of natural gas treatment prior to its transportation/processing [1]. In addition, CO<sub>2</sub> capture from energy industry off-gases serves as a common measure to combat climate change by limiting carbon dioxide emissions [2, 3].

Chemical absorption using aqueous solutions of alkanolamines such as monoethanolamine (MEA), methyl diethanolamine (MDEA), and others is a mature technique for removing CO<sub>2</sub> and H<sub>2</sub>S from natural gas that demonstrates a high removal degree (>95%) of acid gases within a wide range of their partial pressures [4–7]. A key drawback of this technique is degradation (deactivation) of amine solvents [8, 9] due to destruction

of alkanolamines and their involvement in side chemical reactions. This is caused by high temperatures in acid gas desorption units (100–140°C) and, fairly often, by the presence of oxygen in the mixture (up to 10 vol % in flue gases). Therefore, carboxylic acids, amides, amines, aldehydes, ammonia, etc. are formed [10]. Formic, acetic, glycolic, oxalic, and other acids, which are produced in the final step of many chemical transformations of alkanolamines, predictably dominate in the degradation products [10–12]. Furthermore, equipment corrosion and/or low-quality makeup water likely cause amines to react with impurities that are contained both in the feed gas mixture (e.g., sulfur and nitrogen oxides) and in the absorption liquids themselves [7]. This increases the concentration of heat-stable salts (HSS), i.e. salts of protonated alkanolammonium and organic and inorganic acids [13, 14] that do not decompose during

CO<sub>2</sub> desorption under high temperatures [11, 15]. The accumulated HSS markedly impair the sorption capacity of the amine solvent, affect its physicochemical properties, and dramatically increase an equipment corrosion [7, 16].

There have been a number of review studies focused on the existing HSS removal methods [12–14]. The common method for solvent reclaiming from HSS is distillation [8, 17], though alternative techniques exist and include—removal of HSS anions using ion-exchange resins [18, 19], capacitive deionization [20, 21], concentration of HSS using nanofiltration [22, 23], and electromembrane treatment methods [24–26]. Direct and bipolar electrodialysis are applicable for treating MEA-based post-combustion CO<sub>2</sub> capture solvents [27–32] and diethylamine recovery with simultaneous acid production [33, 34].

A novel method for HSS extraction with hydrophobic organic extractants has been recently described [35, 36]. This method enabled the researchers to extract HSS despite their low concentration (1000 ppm) with minimized energy consumption. They used solutions of amines or quaternary ammonium salts with bulky substituents ( $C \geq 8$ ) in higher alcohols ( $C \geq 6$ ) immiscible with amine-based solvents. Tricaprylmethylammonium hydroxide in 1-octanol was shown to bind HSS according to an acid–base mechanism [35], and its efficiency can be enhanced by using branched 2-ethyl-1-hexanol instead of 1-octanol [36].

Like other extraction processes [37], extraction of HSS requires effective contact between the solvent and the extractant. Although achieving the best efficiency, centrifugal extractors exhibit the highest energy consumption, with most of the mixing energy being spent on heating the phases [38]. Conventional mix-settlers have large weight–size parameters [39] and, hence, the longest phase separation time. Extraction columns also have major drawbacks, including the challenges of back-mixing of phases, flooding effect, and poor operating stability under variation of process conditions.

The implementation of mass transfer in membrane modules [40] appears to be an attractive alternative solution to the above challenges. Particularly promising is perstraction (membrane extraction), a method that combines HSS mass transfer across the membrane followed by HSS extraction extraction, which provides for the extractant flowing over the outlet surface of the membrane. In this case, the extractant ensures

selective extraction of the desired component, while the membrane acts as a phase contact surface and prevents the phases from being mixed. Membrane contactors are compact and modular due to their high specific mass transfer area per unit of the contactor volume. Furthermore, membrane contactors provide high energy efficiency (only circulation of phases is necessary) and eliminate the operational challenges typical of extraction columns due to independent control of phase flows [39, 41, 42]. Our research team has demonstrated the advantages of membrane contactors in a number of prior studies focusing on carbon dioxide separation [43–45] and membrane absorption of olefins from their mixtures with paraffins [46, 47].

The perspective of of membrane extraction systems have also been confirmed by relevant studies within field of extraction of carboxylic acids from fermentation broths [48–53]. Therefore, the removal of HSS from aqueous alkanolamine solvents used for the removal of CO<sub>2</sub> and H<sub>2</sub>S appears a logical and relevant application for the perstraction method. However, to the best of the authors' knowledge, there are no available studies for this purpose, whereas relevant works have omitted any discussion on the compatibility of the membranes with organic extractants.

The aim of the present study was to investigate the stability of various industrial and laboratory membranes when exposed to perstraction liquids (i.e., the amine solvent and components of the organic extractant) and to demonstrate, using a model MEA solvent, the basic feasibility of the perstraction of HSS anions.

## EXPERIMENTAL

**Materials.** A 30 wt % MEA aqueous solution (CP grade, ChimMed, Russia) was used as a model CO<sub>2</sub> capture solvent. The presence of HSS in the solution was simulated by adding formic acid (CP grade, ChimMed) until 2.3 g/L (0.05 M) a typical HSS content in post-combustion CO<sub>2</sub> capture solvent [30], was reached. To prepare an HSS extractant, 1-octanol (99%, 360562-1L, Sigma-Aldrich) and methyltrioctylammonium chloride (Aliquat® 336, 50393145, Lot 38-022-14, BASF) were taken. All reactants were used without further purification.

Industrial flat porous polypropylene (PP) and polyvinylidene fluoride (PVDF) membranes, as well as laboratory polysulfone (PSf) membrane samples prepared as described below, were chosen. The membrane characteristics are presented in Table 1.

**Table 1.** Membrane characteristics

Sample	Properties						
	material	grade	manufacturer	structure	standard dimension, mm×mm	pore size, $\mu\text{m}$	thickness, $\mu\text{m}$
PP	Polypropylene	Polysep <sup>tm</sup>	GVS North America (USA)	Symmetric	200×200	0.1 <sup>a</sup>	95
PVDF	Polyvinylidene fluoride	Immobilon®-p	EMD Millipore Corporation (USA)	Symmetric	265×3750	0.45 <sup>a</sup>	127
PSf	Polysulfone	–	–	Asymmetric		0.003 <sup>b</sup>	112

<sup>a</sup> Pore size specified by the manufacturer.

<sup>b</sup> Pore size measured by liquid–liquid displacement porosimetry.

**Fabrication of PSf membranes.** To prepare PSf membrane samples, we used polysulfone (BASF Ultrason® S 6010) pellets and N-methylpyrrolidone (Acros Organics, 99% extra pure, abbreviated as “MP”) as a solvent. Polyethylene glycol with a mean molecular weight of 400 g/mol (PEG-400, Acros Organics) was used as a pore-forming additive.

To prepare a casting solution, the PSf and PEG-400 (1 : 1.25 w/w) were placed in a thermostated reactor and stirred at 150 rpm at 50°C. MP was then added, as the stirring was speeded up to 500 rpm. Under these conditions, the casting solution was stirred for 24 h. The PSf concentration in the solution was 23.9 wt %. Next, the casting solution was filtered at 1.8–2 bar nitrogen through a 4–5  $\mu\text{m}$  stainless steel mesh at 50°C, cooled to room temperature, and vacuum-degassed.

To fabricate the membranes by a phase inversion technique, a 200- $\mu\text{m}$ -thick layer of the polymer solution was casted by a scraping knife onto an acetone-pretreated glass plate and immersed into a non-solvent bath filled with distilled water with a temperature of 20°C. The fabricated asymmetric membranes were water-washed for 24 h, then successively held in ethanol and *n*-hexane (for 2 h each) to prevent the pores from capillary contraction [54], followed by air drying.

**Characterization of membrane stability under contact with process liquids.** The stability of the membranes under the test liquids was evaluated. To this end, the membranes were immersed in a 30 wt % MEA aqueous solution, 1-octanol, and Aliquat® 336 for about 600 h.

Potential chemical transformations of the membrane materials were examined on an IFS-Bruker 66/Vs vacuum FT-IR spectrometer in the reflection mode with a ZnSe crystal (100 scans at a resolution of 4  $\text{cm}^{-1}$ ). The measurements were taken in the range of 4000–400  $\text{cm}^{-1}$  and processed using the Bruker OPUS 6.0 software package.

Potential variations in membrane morphology were examined by scanning electron microscopy (SEM) on a Phenom XL G2 Desktop SEM instrument (Thermo Fisher, USA) equipped with an energy dispersive X-ray spectroscopy (EDS) module. Cleaved membrane samples were prepared, after isopropanol preimpregnation, by cryogenic fracturing in liquid nitrogen, followed by cathodic sputtering of gold (5 nm thick) in a Thermo Fischer Scientific Cressington 108 Auto Sputter Coater (under vacuum of about 0.01 mbar). The SEM accelerating voltage was 15 keV. The average selective layer thickness was derived from micrographs using Gwyddion software (ver. 2.53).

The contact angles were measured by a conventional sessile drop technique using an *LK-1* goniometer (RPC OpenScience Ltd, Russia). All measurements were conducted at room temperature (23±2°C). The contact angle was computed as the arithmetic mean of five measurements. For capturing and digital processing of drop images, DropShape software was used providing Young–Laplace contact angle calculations. The measurement error was 2°.

The surface energy was evaluated by the Owens–Wendt method [55]. This method determines the surface energy ( $\sigma$ ) as a sum of the polar component ( $\sigma^p$ ) and the

**Table 2.** Specification of test liquids [56]

Liquid	Total surface energy $\sigma_{\text{total}}$ , mJ/m <sup>2</sup>	Dispersive component $\sigma^d$ , mJ/m <sup>2</sup>	Polar component $\sigma^p$ , mJ/m <sup>2</sup>
Water	72.8	21.8	51.0
Diiodomethane	50.8	50.8	0.0

dispersive component ( $\sigma^d$ ) using two different liquids. The correlation between the surface energy and equilibrium contact angle of the liquid deposited onto the solid surface is derived from the Fowkes equation:

$$\sigma_l (1 + \cos\theta) = 2(\sigma_l^d \sigma_s^d)^{1/2} + 2(\sigma_l^p \sigma_s^p)^{1/2}, \quad (1)$$

where the superscripts  $d$  and  $p$  refer to the dispersive and polar components of the surface energies of the test liquid ( $\sigma_l$ ) and membrane surface ( $\sigma_s$ ), respectively. Water and diiodomethane were used as test liquids as their application for this purpose has been widely described in published reports [56, 57]. The surface energy components of these liquids are specified in Table 2.

The pore size distribution of the membranes was measured by liquid–liquid displacement porosimetry using a POROLIQ 1000 ML porometer (Porometer, Belgium). This instrument measures the permeance of a membrane with its pores filled with a wetting liquid as a function of the transmembrane pressure applied when a displacing liquid, immiscible with the wetting liquid, is pushed through the membrane [58]. As the transmembrane pressure increases, the wetting liquid is displaced from the pores, thus providing a flow through these pores. The open-pore diameter ( $d_p$ ) is related to the transmembrane pressure through the Young–Laplace equation:

$$d_p = 4\gamma \cos \theta / \Delta p, \quad (2)$$

where  $\gamma$  is the interfacial tension between the two liquids;  $\theta$  is the contact angle between the membrane surface and the wetting liquid (assuming full wetting:  $\cos \theta = 1$ ); and  $\Delta p$  is the transmembrane pressure. The interfacial tension ( $\gamma$ ) for an isobutanol/water mixture is 2.0 mN/m at 20°C.

Using the Young–Laplace equation (2), the transmembrane pressure can be converted to the size of the pores from which the wetting liquid was displaced at this pressure, and the permeance increase can easily be converted into the number of pores of the corresponding size via the Hagen–Poiseuille equation. The wetting liquid

was displaced by gradually raising the transmembrane pressure, with the flow through the membrane being monitored at each pressure applied after 180 s (initial stabilization point). The measurements continued until a linear flow–pressure relationship was reached, indicating that the wetting liquid was completely displaced. The measurements were taken at 20°C using a pair of immiscible liquids prepared by stratification of the isobutanol/water mixture. The water-saturated isobutanol and isobutanol-saturated water were used as wetting and displacing liquids, respectively. Before the measurement, at least three samples (2 cm in diameter) were cut from each membrane and placed in a wetting liquid cup at 20°C for at least 48 h. The membrane pore size was evaluated by averaging the sizes of at least three samples cut from the membrane.

The main criterion to compare membranes was the flow-averaged pore size. This value is normally estimated for the transmembrane pressure required to reach 50% of the maximum permeability. As it takes into account the higher contribution of larger pores to the flow rate, the flow-averaged pore size exceeds the average pore size.

**Model experiments on HSS perstraction from aqueous MEA solution.** For the perstraction experiments, the diffusion cell schematically shown in Fig. 1 was used. The cell was fabricated from polytetrafluoroethylene stable under most organic solvents. The cell consisted of two chambers partitioned by a disk-shaped membrane with an effective area of 12.6 cm<sup>2</sup>. The membrane was sealed by two rubber rings. The containment of the system with the membrane installed was ensured by fastening two coupled chambers at the clamp bracket. Magnetic stir bars were placed in the lower part of the chambers to stir the liquids and, thus, prevented them from concentration polarization. An Ika® electromagnetic stirrer was used as a drive for rotation of the stir bars. To minimize liquid losses due to evaporation, the cells were covered with lids perforated in the center with 2-mm holes. These holes were needed to fill the cells with process fluids (test liquids) and to sample the solutions for analysis. During the experiment, these holes were also covered.

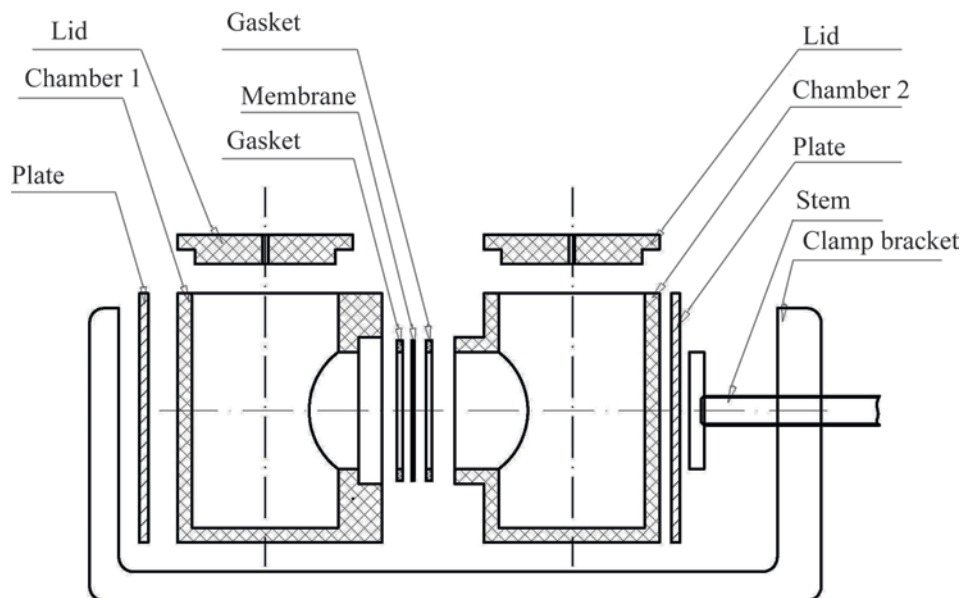


Fig. 1. Diffusion cell setup.

At the beginning of the experiment, 100 mL of the 30 wt % MEA aqueous solution with 0.05 M of formic acid was poured into the left chamber (chamber 1, Fig. 1), and 100 mL of the 1 M OH-modified methyltriethylammonium (Aliquat® 336) solution in 1-octanol was placed in the right chamber (chamber 2). The Aliquat® 336 had been modified in accordance with the procedure described in [35]. The liquids were poured simultaneously into both chambers.

The recovery of formic acid from the aqueous MEA solution was tested at room temperature ( $23 \pm 2^\circ\text{C}$ ) with the solutions in both membrane-partitioned cell chambers being continuously stirred. The formic acid content was controlled by ion-exchange chromatography using an Aquilon-Stayer-1 system equipped with a Shodex ICSI-50 4E column (with 3.2 mmol of  $\text{NaHCO}_3$  and 0.1 mmol of  $\text{Na}_2\text{CO}_3$  as eluents), an EMCES 21 electric suppressor, and a CD-510 conductometric detector.

## RESULTS AND DISCUSSION

A membrane extraction system cannot function effectively unless the membranes are compatible with the contacting liquids. In other words, the membranes must be chemically and morphologically stable under the contacting liquids. To test the compatibility, the membranes were exposed to prolonged contact (see above) with the model absorbent (30 wt % MEA

aqueous solution), as well as with 1-octanol and modified methyltriethylammonium (Aliquat® 336) as the selective extractant's components. After the exposure, the membrane samples were examined using a number of physicochemical analytical methods.

**Chemical stability of membrane materials in process liquids.** Figure 2 shows the IR spectra of the initial membranes as well as of the samples exposed to 30 wt % MEA, 1-octanol, and Aliquat® 336 for 600 h. We see that the IR spectra of the initial and treated samples are almost identical for all the membrane materials studied (PP, PVDF, and PSf).

It can be concluded that the prolonged exposure to the MEA solution, 1-octanol, and Aliquat® 336 caused no significant chemical degradation of the membranes. This suggests that the tested membranes were chemically compatible with the tested liquids.

### *Morphological Stability of Membranes under Process Fluids*

**SEM data.** The structural stability of the membranes exposed to the test liquids for 600 h was examined by the SEM method. An analysis of the surface and cross-section of the PVDF and PSf membranes (Tables 3 and 4, respectively) suggested that the membrane structures remained largely unchanged even after their prolonged contact with the MEA solution, 1-octanol,

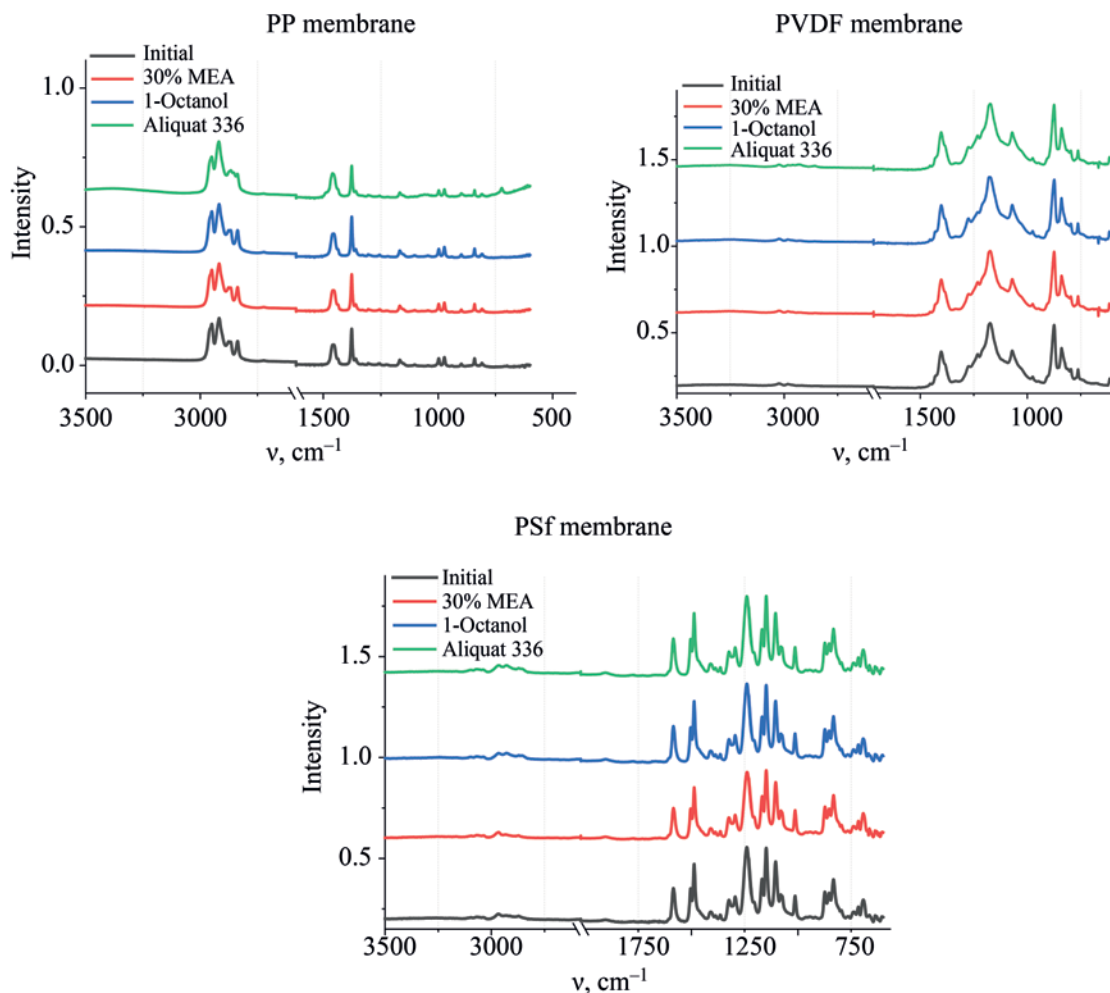


Fig. 2. IR spectra of initial membranes and samples exposed to 30 wt % MEA, 1-octanol, and Aliquat® 336 for 600 h.

and Aliquat® 336. In addition to the differences in the particular polymeric materials (partially crystalline fluorine-containing thermoplastic PVDF vs. amorphous thermoplastic PSf), these membranes had dissimilar porous structures: a symmetric spongy porous structure for PVDF (see Table 3) versus an asymmetric structure with two fine-pore selective layers on both side surfaces and finger-like macrovoids in the cross-section for PSf (see Table 4). Table 4 clearly shows that the SEM resolution proved insufficient to measure the size of the PSf surface pores. A comparison of the micrographs before and after the exposure to the test liquids indicates the morphological stability of the membranes.

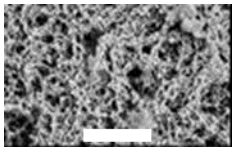
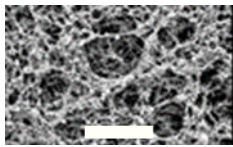
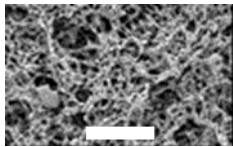
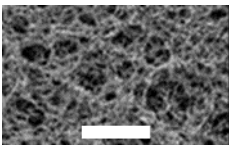
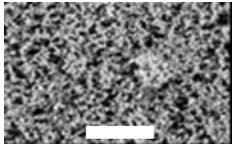
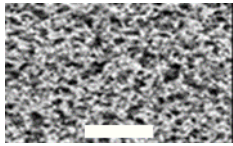
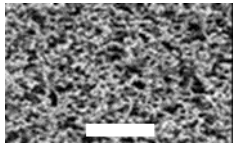
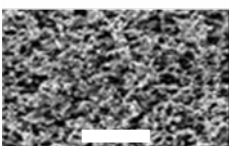
On the other hand, the micrographs of the PP membrane surface (Table 5) show that the membrane pores were narrowed after the prolonged contact of the symmetric PP membrane with the MEA solution and

Aliquat® 336. However, the prolonged exposure of the PP membrane to 1-octanol had no noticeable effect on its porous morphology, like in the cases of PVDF and PSf. The pore size aspects are discussed in the next subsection.

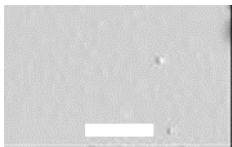
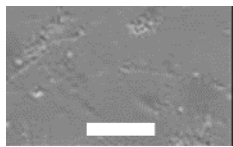
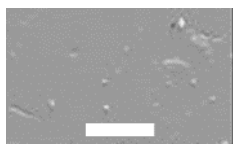
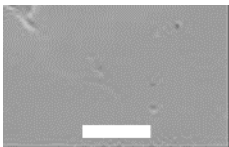
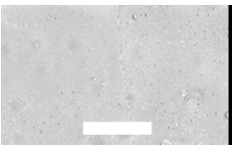
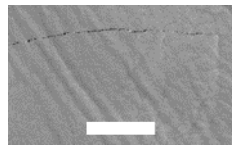
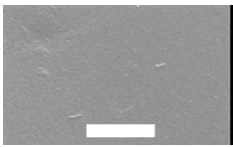
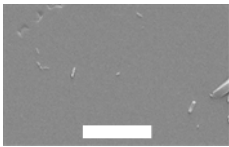
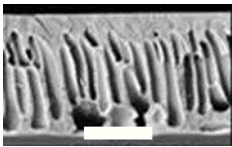
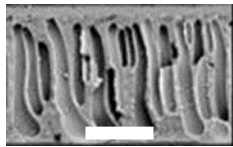
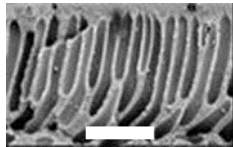
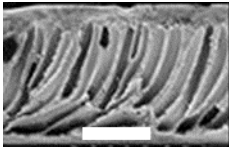
#### *Evaluation of Membrane Pore Size*

The porous structure of PSf, PVDF, and PP membranes before and after the solvent exposure were examined by liquid porosimetry. Table 6 shows the flow-averaged pore size of the membranes before and after the exposure to the test liquids. In the cases of PSf and PVDF, the exposure to 30% MEA and Aliquat® 336 did not affect the pore size. Some changes were observed when these membranes, especially PSf, were exposed to 1-octanol. However, these effects were far below those for the PP membrane samples after their prolonged contacts with 30% MEA and Aliquat® 336 (in these cases, the pore sizes were

**Table 3.** PVDF membrane porous structure (symmetric)

Parameter	Initial	After solvent exposure		
		30% MEA	1-octanol	Aliquat® 336
Surface 1 (15 $\mu\text{m}$ scale)				
Cross-section (15 $\mu\text{m}$ scale)				

**Table 4.** PSf membrane porous structure (asymmetric)

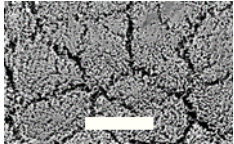
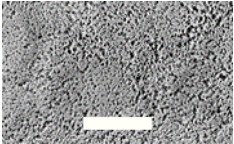
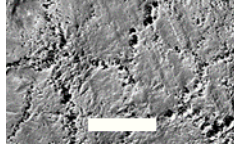
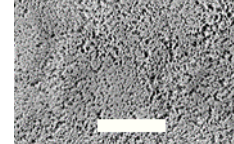
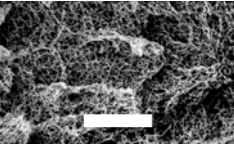
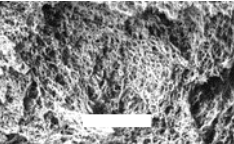
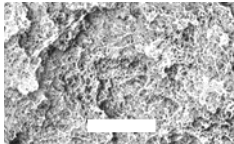
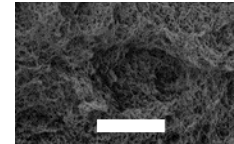
Parameter	Initial	After solvent exposure		
		30% MEA	1-octanol	Aliquat® 336
Surface 1 (15 $\mu\text{m}$ scale)				
Surface 2 (15 $\mu\text{m}$ scale)				
Cross-section (50 $\mu\text{m}$ scale)				

reduced by 30 and 40%, respectively). On the other hand, the prolonged contact of the PP membrane with 1-octanol did not affect the pore size or the pore size distribution. Importantly, the porosimetry revealed narrowing of PP membrane pores after their contact with the MEA solution and Aliquat® 336, as well as their invariability after the

1-octanol exposure, corroborate well with the SEM data on the membrane morphology (see Table 5).

Thus, in terms of the morphological stability of the tested membranes, PVDF and PSf proved to be the more promising for the of HSS perstraction proof-of-concept. Although PP membranes also proved feasible,

**Table 5.** PP membrane porous structure (symmetric)

Parameter	Initial	After solvent exposure		
		30% MEA	1-octanol	Aliquat® 336
Surface 1 (15 µm scale)				
Cross-section (15 µm scale)				

**Table 6.** Flow-averaged pore size in membrane samples

Membrane sample	Flow-averaged pore size, nm			
	30% MEA	Aliquat® 336	1-octanol	initial
PSf	3.5	3.5	4.7	3.3
PVDF	770	780	730	780
PP	170	150	240	250

**Table 7.** Water permeance of membranes

Membrane sample	Water permeance, L m <sup>-2</sup> h <sup>-1</sup> atm <sup>-1</sup>			
	30% MEA	Aliquat® 336	1-octanol	initial
PSf	1.3	1.3	1.6	1.2
PVDF	28300	29400	28000	28700
PP	1120	830	1520	1550

the performance of the PP membrane contactor system may decline over time if their porous structure is affected when exposed to a selective extractant.

**Transport properties of membranes.** The transport properties of the membranes were characterized in terms of water permeance (Table 7). The data clearly show an immense difference (by several orders of magnitude) in the permeance between the tested membranes. In particular, the PVDF permeance was about one order of magnitude higher than that of the PP membranes, and more than four orders of magnitude higher than the PSf permeance. It is also worth noting that the water permeance through PVDF was not affected by the

prolonged exposure of this membrane to aqueous MEA, Aliquat® 336, and 1-octanol. This gets in line with the SEM micrographs (see Table 3) and the flow-averaged pore sizes (see Table 6), indicating the stability both of the membrane morphology and pore size after the contact with the process fluids.

In the case of PSf membrane, the water permeance increased by 30% after the prolonged exposure to 1-octanol. This concurs with the increase in the PSf pore size after the prolonged 1-octanol exposure (see Table 6). Specifically, the flow-averaged pore size of the PSf membrane rose from 3.3 to 4.7 nm.



**Table 8.** Contact angles and surface energies of membrane samples before and after liquid treatment

Membrane sample	Treatment	$\theta$ water, deg	$\theta$ CH <sub>2</sub> I <sub>2</sub> , deg	$\sigma_s^p$ , mJ/m <sup>2</sup>	$\sigma_s^d$ , mJ/m <sup>2</sup>	$\sigma_s$ , mJ/m <sup>2</sup>
PVDF	Initial	123	96	0.1	9.3	9.4
	30% MEA	120	95	0.3	9.5	9.8
	1-Octanol	123	93	0.1	10.6	10.7
	Aliquat® 336	0	0	35	40	75
PP	Initial	129	75	1	21	22
	30% MEA	125	98	0.1	8.6	8.7
	1-Octanol	117	89	0.3	11.8	12.1
	Aliquat® 336	0	35	46	27	73
PSf	Initial	76	17	4.5	41.5	46
	30% MEA	68	19	8.5	39.5	48
	1-Octanol	80	20	3.6	41.4	45
	Aliquat® 336	23	18	34	36	70

**Table 9.** Contact angles of membranes with test liquids

Liquid	$\theta$ , deg		
	PSf	PVDF	PP
Aqueous MEA (30 wt %) + 0.05 M HCOOH	79.7	0	44.6
1 M Aliquat® 336 in 1-octanol	22.0	18.7	10.9

The test of the PP membrane also yielded coherent results. Given the reduced pore size (see the SEM images in Table 5 and the liquid porosimetry data in Table 6), the exposure of the PP membrane to 30% MEA and Aliquat® 336 predictably lowered the water permeance from 250 to 170 L m<sup>-2</sup> h<sup>-1</sup> atm<sup>-1</sup> and 150 L m<sup>-2</sup> h<sup>-1</sup> atm<sup>-1</sup>, respectively.

**Surface properties of membranes.** The water and diiodomethane contact angles of the initial membranes and the samples exposed to the process liquids are presented in Table 8. Except for the samples exposed to Aliquat® 336, the dispersive component made a predominant contribution to the surface energy. The polar component ranged from 0.1 to 8.5 mJ/m<sup>2</sup>, and the total surface energy from 8.7 to 48 mJ/m<sup>2</sup>. This pattern is generally typical for hydrophobic materials. Bahriamian [59] reports data on commercial bitumen samples with contact angles of 100.5°–103.8°: the polar component ranges between 0.3 and 0.9 mJ/m<sup>2</sup>, and the dispersive component between 23.8 and 33.1 mJ/m<sup>2</sup>. Saïdi et al. [60] provide surface energy data for copolymers of perfluorooctyl acrylate C<sub>8</sub>F<sub>17</sub>–(CH<sub>2</sub>)<sub>n</sub>OC(O)CH=CH<sub>2</sub> and butyl acrylate (with water contact angles of 98°–123°): 0–5 mJ/m<sup>2</sup> for the

polar component and 4.3–25.3 mJ/m<sup>2</sup> for the dispersive component.

The presented data clearly show that immersion the samples in Aliquat® 336 hydrophilized the membrane surfaces, as indicated by the significant drop in the contact angles and the rise in the surface energies. As a consequence, during the operation of the membrane contactor system, the membrane pores were likely filled with the selective extractant first.

Thus, the studied membranes proved to be compatible with the process liquids (30 wt % MEA, 1-octanol, and Aliquat® 336); hence, these membrane materials are promising candidates to demonstrate the feasibility of HSS perstraction from alkanolamine solutions using a methyltrioctylammonium hydroxide solution in 1-octanol as an extractant.

Table 9 presents the contact angles of PSf, PVDF, and PP membranes with the test liquids during the HSS perstraction from the degraded alkanolamine solution: 30 wt % MEA + 0.05 M HCOOH as a solution to be treated, and 1 M Aliquat® 336 in 1-octanol as an extractant. The data clearly show that the PVDF

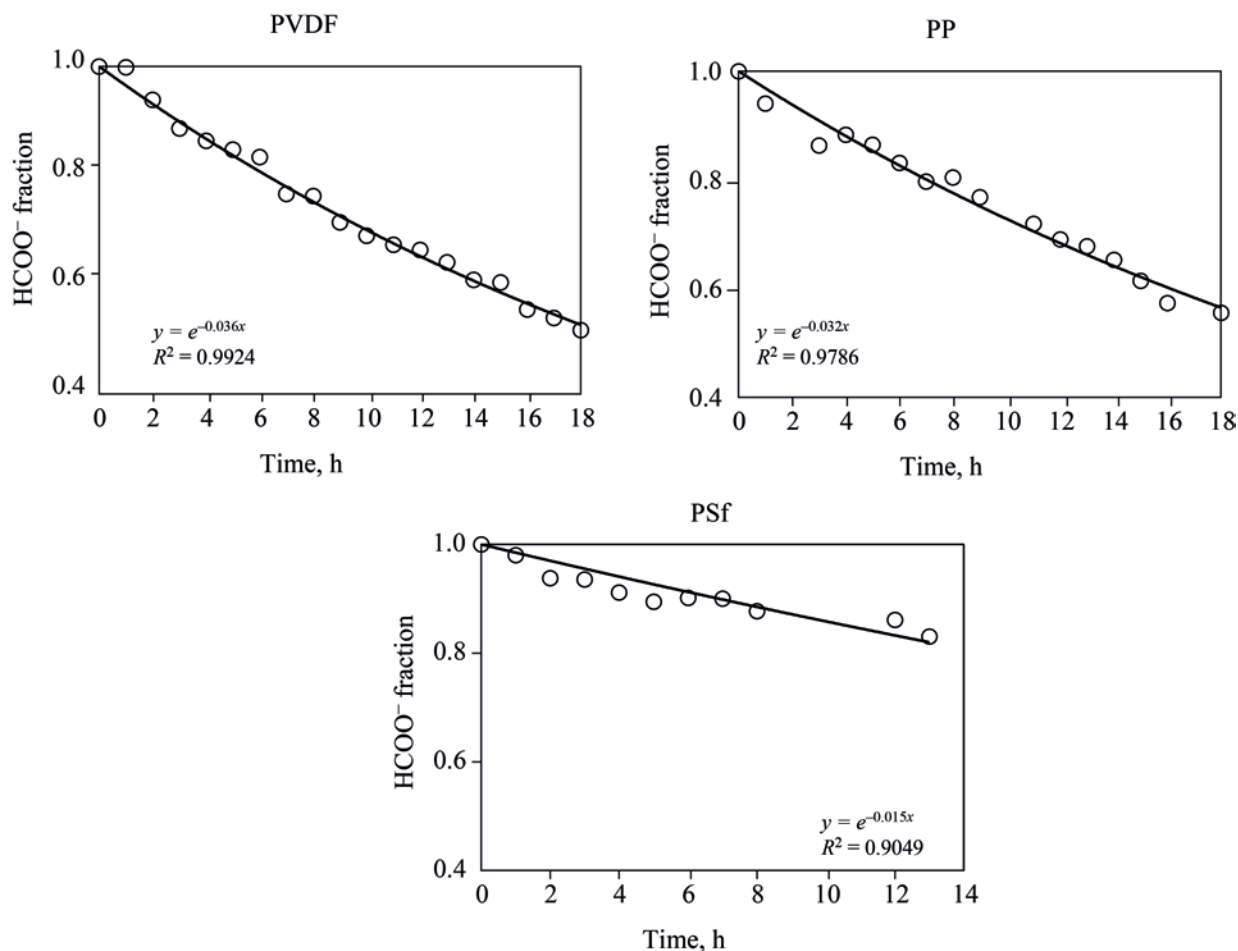


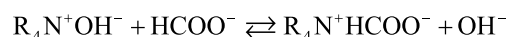
**Fig. 3.** Perstraction test data for different membrane materials: dots refer to experimental data, and lines show exponential approximation. The content of formic acid is presented as relative concentration ( $C_t/C_0$ ).

membrane was completely wetted with the aqueous MEA solution. Therefore, it would be fair to assume that, when the process fluids came in contact with the membrane in the perstraction cell (Fig. 1), the membrane pores were filled with the aqueous MEA solution containing 0.05 M of formic acid as an HSS model. In contrast, the porous structure of the PSf and PP membranes was most likely filled with the extractant (the 1 M Aliquat® 336 solution in 1-octanol).

**Perstraction transport of formate ions.** The perstraction test data for each membrane are illustrated in Fig. 3.

Formic acid diffused from the left chamber of the diffusion cell (2.3 g/L, or 0.05 M in the aqueous MEA solution) through the membrane into the right chamber, and interacted with the active component of the Aliquat® 336 extractant (the 1 M solution in 1-octanol)

according to the ion exchange reaction, where R is  $\text{C}_8\text{H}_{17}$  or  $\text{CH}_3$  [35]:



Since an excess amount of the extractant was used, this reaction can be considered as a first-order reaction and described by an exponential function (see Fig. 3). The effective reaction rate constants were found to range between 0.03 and 0.04  $\text{h}^{-1}$  for perstraction through PVDF and PP membranes. The approximation of the experimental data proved to be satisfactory (with a correlation coefficient  $R^2$  above 0.97). The only exception was the PSf membrane case, with  $R^2$  equal to about 0.9, which may be associated with an additional resistance to mass transfer due to the asymmetry of PSf membranes, with fine-pore layers on both sides.

Thus, the test data convincingly show the proof-of-concept of HSS perstraction from aqueous MEA solutions for all the studied membranes. The PVDF membranes achieved the best performance: in the perstraction experiment, up to 50% of formic acid was extracted over the 18 h of experiment. In this case, no direct phase dispersion was observed, nor was a stable emulsion formed (which usually appears under direct contact of a MEA solution with this extractant). Despite the comparable performance demonstrated by the PP membranes, they require additional experiments to test prolonged operation of a membrane extraction system and identify the effects of pore size changes (see Tables 5 and 6) on the process performance.

### CONCLUSIONS

This study proposes a perstraction (membrane extraction) method for the removal of heat-stable salts (HSS) from alkanolamine CO<sub>2</sub> solvents (based on monoethanolamine) using industrial polypropylene (PP) and polyvinylidene fluoride (PVDF) membranes, as well as laboratory polysulfone (PSf) membranes. Using IR spectrometry and scanning electron microscopy, the PVDF and PSf membrane samples were found to be chemically and morphologically stable when exposed for at least 600 h to a model solvent (30 wt % MEA aqueous solution) and to the components of a selective HSS extractant, namely 1-octanol and methyltrioctylammonium chloride (Aliquat® 336). Using liquid–liquid displacement porosimetry, it was shown that prolonged contact with Aliquat® 336 and 30 wt % MEA narrowed the PP membrane pores from 250 nm to 150–170 nm, thus impairing their transport properties (indicated by the 1.4–1.9-fold drop in the water permeance).

The surface properties of the membranes were further evaluated. Using the formate anion transport from the 30 wt % MEA aqueous solution to an OH-modified Aliquat® 336 solution in 1-octanol, the study demonstrated the proof-of-concept of HSS perstraction from alkanolamine solvents without direct phase dispersion or emulsion formation for the tested membrane materials. The formic acid content in the solvent during the perstraction experiments was described by an exponential function, with the effective reaction rate constants ranging between 0.03 and 0.04 h<sup>-1</sup> for

perstraction through PVDF and PP membranes. Among the tested membrane materials, PVDF membranes exhibited the highest performance: up to 50% of formic acid was extracted from the model solvent over 18 h.

### AUTHOR INFORMATION

M.I. Kostyanaya, ORCID: <https://orcid.org/0000-0001-8192-3824>

A.A. Yushkin, ORCID: <https://orcid.org/0000-0002-0118-1515>

D.S. Bakhtin, ORCID: <https://orcid.org/0000-0001-8619-8326>

S.A. Legkov, ORCID: <https://orcid.org/0000-0001-9739-4891>

S.D. Bazhenov, ORCID: <https://orcid.org/0000-0002-2010-5294>

### ACKNOWLEDGMENTS

This work was performed using equipment of the Center for Collective Use “TIPS RAS Analytical center of deep oil processing and petrochemistry.” The authors thank A.V. Balyinin for his kind cooperation in the liquid–liquid displacement porosimetry experiments.

### FUNDING

The study was funded by Grant no. MK-4659.2021.4 of the President of the Russian Federation.

### CONFLICT OF INTEREST

The authors declare no conflict of interest requiring disclosure in this article.

### OPEN ACCESS

This article is licensed under a Creative Commons Attribution 4.0 International License, which permits use, sharing, adaptation, distribution and reproduction in any medium or format, as long as you give appropriate credit to the original author(s) and the source, provide a link to the Creative Commons license, and indicate if changes were made. The images or other third party material in this article are included in the article’s Creative Commons license, unless indicated otherwise in a credit line to the material. If material is not included in the article’s Creative Commons license and your intended use is not permitted by statutory regulation or exceeds the permitted use, you will need to obtain permission directly

from the copyright holder. To view a copy of this license, visit <http://creativecommons.org/licenses/by/4.0/>.

## REFERENCES

- Kohl, A. and Nielsen, R., *Gas Purification*, Huston, TX: Gulf Publishing Company, 1997, 5 ed.
- Chao, C., Deng, Yi., Dewil, R., Baeyens, J., and Fan, X., *Renew. Sus. Energy Rev.*, 2021, vol. 138, p. 110490. <https://doi.org/10.1016/j.rser.2020.110490>
- Alent'ev, A.Yu., Volkov, A.V., Vorotyntsev, I.V., Maksimov, A.L., and Yaroslavtsev, A.B., *Membran. Membran. Technol.*, 2021, vol. 3, pp. 255–273. <https://doi.org/10.1134/S0965544120010089>
- Borhani, T.N. and Wang, M., *Renew. Sus. Energy Rev.*, 2019, vol. 114, p. 109299. <https://doi.org/10.1016/j.rser.2019.109299>
- Rochelle, G.T., *Science*. 2009, vol. 325, no. 5948, pp. 1652–1654. <https://doi.org/10.1126/science.1176731>
- Anufrikov, Y.A., Kuranov, G.L., and Smirnova, N.A., *Russ. J. Appl. Chem.*, 2007, vol. 80, no. 4, pp. 515–527. <https://doi.org/10.1134/S1070427207040015>
- Bazhenov, S.D., Novitskii, E.G., Vasilevskii, V.P., Grushevenko, E.A., Bienko, A.A., and Volkov, A.V., *Russ. J. Appl. Chem.*, 2019, vol. 92, no. 8, pp. 1045–1063. <https://doi.org/10.1134/S1070427219080019>
- Golubeva, I.A., Dashkina, A.V., and Shulga, I.V., *Petrol. Chem.*, 2020, vol. 60, pp. 45–50. <https://doi.org/10.1134/S0965544120010089>
- Buvik, V., Høisæter, K.K., Vevelstad, S.J., and Knuutila, H.K., *Int. J. Greenh. Gas Control.*, 2021, vol. 106, p. 103246. <https://doi.org/10.1016/j.ijggc.2020.103246>
- Gouedard, C., Picq, D., Launay, F., and Carrette, P.L., *Int. J. Greenh. Gas Control.*, 2012, vol. 10, pp. 244–270. <https://doi.org/10.1016/j.ijggc.2012.06.015>
- Supap, T., Saiwan, C., Idem, R., and Tontiwachwuthikul, P.P.T., *Carbon Manag.*, 2011, vol. 2, no. 5, pp. 551–566. <https://doi.org/10.4155/cmt.11.55>
- Dumée, L., Scholes, C., Stevens, G., and Kentish, S., *Int. J. Greenh. Gas Control.*, 2012, vol. 10, pp. 443–455. <https://doi.org/10.1016/j.ijggc.2012.07.005>
- Elmoudir, W., Supap, T., Saiwan, C., and Idem, R., *Carbon Manag.*, 2012, vol. 3, no. 5, pp. 485–509. <https://doi.org/10.4155/cmt.12.55>
- Wang, T., Hovland, J., and Jens, K.J., *J. Environ. Sci.*, 2015, vol. 27, pp. 276–289. <https://doi.org/10.1016/j.jes.2014.06.037>
- Feron, P.H.M., *Absorption-Based Post-combustion Capture of Carbon Dioxide*, Woodhead Publishing., 2016. <https://doi.org/10.1016/c2014-0-03382-5>
- Ling, H., Liu, S., Gao, H., and Liang, Z., *Sep. Purif. Technol.*, 2019, vol. 212, pp. 822–833. <https://doi.org/10.1016/j.seppur.2018.12.001>
- Tavan, Y., Moradi, M., Rostami, A., and Azizpour, H., *Sep. Purif. Technol.*, 2020, vol. 237, pp. 116314. <https://doi.org/10.1016/j.seppur.2019.116314>
- Bayati, B., Mirshekari, M., Veisy, A., and Gando-Ferreira, L.M., *Chem. Pap.*, 2019, vol. 73, no. 2, pp. 491–500. <https://doi.org/10.1007/s11696-018-0598-0>
- Pal, P., Banat, F., and AlShoaibi, A., *J. Nat. Gas Sci. Eng.*, 2013, vol. 15, pp. 14–21. <https://doi.org/10.1016/j.jngse.2013.08.001>
- Durrani, M., Abu Haija, M., Vengatesan, M.R., Zain, J., Alhseinat, E., and Banat, F., *Int. J. Greenh. Gas Control.*, 2019, vol. 85, pp. 166–173. <https://doi.org/10.1016/j.ijggc.2019.02.019>
- Arora, N., Banat, F., and Alhseinat, E., *Chem. Eng. J.*, 2019, vol. 356, pp. 400–412. <https://doi.org/10.1016/j.cej.2018.09.054>
- Ghorbani, A., Bayati, B., Poerio, T., Argurio, P., Kikhavani, T., Namdari, M., and Ferreira, L.M., *Molecules*, 2020, vol. 25, no. 21, pp. 4911–4926. <https://doi.org/10.3390/molecules25214911>
- Lim, J., Scholes, C.A., Dumée, L.F., and Kentish, S.E., *Int. J. Greenh. Gas Control.*, 2014, vol. 30, pp. 34–41. <https://doi.org/10.1016/j.ijggc.2014.08.020>
- Kikhavani, T., Mehdizadeh, H., Van der Bruggen, B., and Bayati, B., *Chem. Eng. Technol.*, 2021, vol. 44, no. 2, pp. 318–328. <https://doi.org/10.1002/ceat.202000375>
- Wang, Y., Li, W., Yan, H., and Xu, T., *J. Ind. Eng. Chem.*, 2018, vol. 57, pp. 356–362. <https://doi.org/10.1016/j.jiec.2017.08.043>
- Chen, F., Chi, Y., Zhang, M., Liu, Z., Fei, X., Yang, K., and Fu, C., *Sep. Purif. Technol.*, 2020, vol. 242, p. 116777. <https://doi.org/10.5004/dwt.2020.25935>
- Lim, J., Aguiar, A., Scholes, C.A., Dumée, L.F., Stevens, G.W., and Kentish, S.E., *Ind. Eng. Chem. Res.*, 2014, vol. 53, no. 49, pp. 19313–19321. <https://doi.org/10.1021/ie503506b>
- Lim, J., Aguiar, A., Reynolds, A., Pearson, P., Kentish, S.E., and Meuleman, E., *Int. J. Greenh. Gas Control.*, 2015, vol. 42, pp. 545–553. <https://doi.org/10.1016/j.ijggc.2015.09.004>
- Volkov, A., Vasilevsky, V., Bazhenov, S., Volkov, V., Rieder, A., Unterberger, S., and Schallert, B., *Energy Proc.*, 2014, vol. 51, pp. 148–153. <https://doi.org/10.1016/j.egypro.2014.07.016>
- Bazhenov, S., Rieder, A., Schallert, B., Vasilevsky, V., Unterberger, S., Grushevenko, E., Volkov, V., and Volkov, A., *Int. J. Greenh. Gas Control.*, 2015, vol. 42, pp. 593–601. <https://doi.org/10.1016/j.ijggc.2015.09.015>
- Grushevenko, E.A., Bazhenov, S.D., Vasilevskii, V.P., Novitskii, E.G., and Volkov, A.V., *Russ. J. Appl.*

- Chem.*, 2018, vol. 91, no. 4, pp. 602–610.  
<https://doi.org/10.1134/S1070427218040110>
32. Novitsky, E.G., Grushevenko, E.A., Vasilevsky, V.P., and Volkov, A.V., *Membran. Membran. Technol.*, 2020, vol. 2, pp. 109–114.  
<https://doi.org/10.1134/S2517751620020080>
  33. Karpenko, T.V., Kovalev, N.V., Sheldeshov, N.V., and Zabolotsky, V.I., *Membran. Membran. Technol.*, 2022, vol. 4, pp. 59–68.  
<https://doi.org/10.1134/S2517751622010048>
  34. Sheldeshov, N.V., Zabolotsky, V.I., Karpenko, T.V., and Kovalev, N.V., *Membran. Membran. Technol.*, 2020, vol. 2, pp. 189–194.  
<https://doi.org/10.1134/S2517751620030075>
  35. Akkarachalanont, P., Saiwan, C., Supap, T., Idem, R., and Tontiwachwuthikul, P., *Ind. Eng. Chem. Res.*, 2016, vol. 55, no. 17, pp. 5006–5018.  
<https://doi.org/10.1021/acs.iecr.6b00035>
  36. Karnwiboon, K., Krajangpit, W., Supap, T., Muchan, P., Saiwan, C., Idem, R., and Koiwanit, J., *Sep. Purif. Technol.*, 2019, vol. 228, pp. 115744.  
<https://doi.org/10.1016/j.seppur.2019.115744>
  37. Katasonova, O.N., Savonina, E.Yu., and Maryutina, T.A., *Russ. J. Appl. Chem.*, 2021, vol. 94, pp. 411–436.  
<https://doi.org/10.1134/S1070427221040017>
  38. Meikrantz, D.H., Meikrantz, S.B., and Macaluso, L.L., *Chem. Eng. Commun.*, 2001, vol. 188, no. 1, pp. 115–127.  
<https://doi.org/10.1080/00986440108912900>
  39. Song, J., Huang, T., Qiu, H., Niu, X., Li, X.M., Xie, Y., and He, T., *Desalination.*, 2018, vol. 440, pp. 18–38.  
<https://doi.org/10.1016/j.desal.2018.01.007>
  40. Apel, P.Yu., Bobreshova, O.V., Volkov, A.V., Volkov, V.V., Nikonenko, V.V., Stenina, I.A., Filippov, A.N., Yampolskii, Yu.P., and Yaroslavtsev, A.B., *Membran. Membran. Technol.*, 2019, vol. 1, pp. 45–63.  
<https://doi.org/10.1134/S2517751619020021>
  41. Gabelman, A. and Hwang, S.T., *J. Memb. Sci.*, 1999, vol. 159, nos. 1–2, pp. 61–106.  
[https://doi.org/10.1016/S0376-7388\(99\)00040-X](https://doi.org/10.1016/S0376-7388(99)00040-X)
  42. Bazhenov, S.D., Bilydukevich, A.V., Volkov, A.V., *Fibers*, 2018, vol. 6, no. 4, pp. 76.  
<https://doi.org/10.3390/fib6040076>
  43. Dibrov, G.A., Volkov, V.V., Vasilevsky, V.P., Shutova, A.A., Bazhenov, S.D., Khotimsky, V.S., van de Runstraat, A., Goetheer, E.L.V., and Volkov, A.V., *J. Memb. Sci.*, 2014, vol. 470, pp. 439–450.  
<https://doi.org/10.1016/j.memsci.2014.07.056>
  44. Malakhov, A.O. and Bazhenov, S.D., *Petrol. Chem.*, 2018, vol. 58, no. 4.  
<https://doi.org/10.1134/S0965544118040072>
  45. Bazhenov, S., Malakhov, A., Bakhtin, D., Khotimskiy, V., Bondarenko, G., Volkov, V., Ramdin, M., Vlught, T.J.H., and Volkov, A., *Int. J. Greenh. Gas Control.*, 2018, vol. 71, pp. 293–302.  
<https://doi.org/10.1016/j.ijggc.2018.03.001>
  46. Malakhov, A.O., Bazhenov, S.D., Vasilevsky, V.P., Borisov, I.L., Ovcharova, A.A., Bilydukevich, A.V., Volkov, V.V., Giorno, L., and Volkov, A.V., *Sep. Purif. Technol.*, 2019, vol. 219, pp. 64–73.  
<https://doi.org/10.1016/j.seppur.2019.02.053>
  47. Ovcharova, A., Vasilevsky, V., Borisov, I., Bazhenov, S., Volkov, A., Bilydukevich, A., and Volkov, V., *Sep. Purif. Technol.*, 2017, vol. 183, pp. 162–172.  
<https://doi.org/10.1016/j.seppur.2017.03.023>
  48. Gössi, A., Riedl, W., and Schuur, B., *Chem. Eng. Sci.: X*, 2022, vol. 13, pp. 100119.  
<https://doi.org/10.1016/j.cesx.2021.100119>
  49. Gössi, A., Burgener, F., Kohler, D., Urso, A., Kolvenbach, B.A., Riedl, W., and Schuur, B., *Sep. Purif. Technol.*, 2020, vol. 241, p. 116694.  
<https://doi.org/10.1016/j.seppur.2020.116694>
  50. Sofiya, K., Poonguzhali, E., Kapoor, A., Delfino, P., and Prabhakar, S., *J. Membr. Sci. Res.*, 2019, vol. 5, no. 3, pp. 233–239.  
<https://doi.org/10.22079/JMSR.2018.88804.1199>
  51. De Sitter, K., Garcia-Gonzalez, L., Matassa, C., Bertin, L., and De Wever, H., *Sep. Pur. Tech.*, 2018, vol. 206, pp. 177–185.  
<https://doi.org/10.1016/j.seppur.2018.06.001>
  52. Burgé, G., Chemarin, F., Moussa, M., Saulou-Bérion, C., Allais, F., Spinnler, H., and Athès, V., *J. Chem. Tech. Biotech.*, 2016, vol. 91, pp. 2705–2712.  
<https://doi.org/10.1002/jctb.4878>
  53. Grzenia, D.L., Schell, D.J., and Wickramasinghe, S.R., *J. Membr. Sci.*, 2008, vol. 322, pp. 189–195.
  54. Bilydukevich, A.V. and Usosky, V.V., *Petrol. Chem.*, 2014, vol. 54, no. 8, pp. 652–658.  
<https://doi.org/10.1134/S0965544114080027>
  55. Owens, D.K. and Wendt, R.C., *J. Appl. Polym. Sci.*, 1969, vol. 13, pp. 1741–1747.  
<https://doi.org/10.1002/app.1969.070130815>
  56. Guettler, B.E., Moresoli, C., and Simon, L.C., *Ind. Crops Product.*, 2013, vol. 50, pp. 219–226.  
<https://doi.org/10.1016/j.indcrop.2013.06.035>
  57. Arikan, E., Holtmannspötter, J., Zimmer, F., Hofmann, T., and Gudladt, H.J., *Int. J. Adhes. Adhes.*, 2019, vol. 95, p. 102409.  
<https://doi.org/10.1016/j.ijadhadh.2019.102409>
  58. Yushkin, A.A., Efimov, M.N., Malakhov, A.O., Karpacheva, G.P., Bondarenko, G., Marbelia, L., Vankelecom, I.F.J., and Volkov, A.V., *React. Func. Polym.*, 2021, vol. 158, p. 104793.  
<https://doi.org/10.1016/j.reactfunctpolym.2020.104793>
  59. Bahriamian, A., *Degree Project in Highway and Railway Engineering*, Stockholm, Sweden, 2002.
  60. Saïdi, S., Guittard, F., Guimon, C., and Gëribaldi, S., *Macromol. Chem. Phys.*, 2005, vol. 206, no. 11, pp. 1098–1105.  
<https://doi.org/10.1002/macp.200500015>